Porosity of a sea-ice pressure ridge keel estimated on the basis of surface nuclear magnetic resonance measurements

Lasse Rabenstein[1], Andre Nuber[1], Jochen Lehmann-Horn[1], Marian Hertrich[1], Stefan Hendricks[2], Andy Mahoney[3], Hajo Eicken[3]

[1] Institute of Geopyhsics, ETH Zürich, Switzerland
rabenstein@aug.ig.erdw.ethz.ch, nuber@aug.ig.erdw.ethz.ch, jochenl@aug.ig.erdw.ethz.ch, hertrich@aug.ig.erdw.ethz.ch
[2] Alfred Wegener Institute for Polar and Marine Research, Bremerhaven, Germany
Stefan.Hendricks@awi.de
[3] Geophysical Institute, University of Alaska Fairbanks, AK, United States
mahoney@gi.alaska.edu, hajo.eicken@gi.alaska.edu

Introduction

The volume fraction of liquid in sea ice (which typically accounts for well over 90% of the total porosity) is an important physical quantity because it determines the mechanical and transport properties of sea ice and for high-porosity sea ice it is an important component of the ice mass budget. Of particular importance, but poorly studied, is the distribution of pore space and liquid-filled voids in sea-ice pressure ridges. Up to 30% of the Arctic sea ice volume consists of deformed ice in the form of pressure ridges. These are three dimensional and non-consolidated structures built up of crushed ice floes, and are usually between 2 and 20 meters thick. Below sea level larger voids between ice floe fragments and pores (cm to sub-mm scale) in a pressure ridge are filled with seawater or brine, such that its total porosity equals its liquid water content. Determining the volume fraction of these inclusions is of great importance for estimates of the sea-ice mass budget and thickness distribution, as determined by other geophysical measurements, such as electromagnetic induction sounding (EM) or submarine sonar.
A powerful hydrogeophysical method for directly estimating liquid water content (and porosity) is surface nuclear magnetic resonance (surface NMR). The idea of applying surface NMR to aquifer investigations arose in the 1960s but the first effective equipment was not designed and built until the early 1990s. In this study we explore the utility of surface NMR tomography to provide volume integrated measures of liquid water content in sea-ice pressure ridge keels. We further highlight challenges which need to be addressed to make surface NMR a practical sea-ice field tool in the future. A numerical modeling study was performed prior to the field survey, which showed that surface NMR is in theory suitable for determining the water content distribution in pressure ridges. The surface NMR fieldwork and the numerical modeling study are discussed in greater detail in Nuber et al. (2012). In addition to the work of Nuber and co-workers, the present expanded abstract presents the results of an electrical resistivity tomography survey carried out over the same pressure ridge. The method of surface NMR is explained in detail by Hertrich et al. (2008) and will not be repeated here.

Field Survey

For this pioneering application of surface NMR to sea ice, we chose a first year sea-ice pressure ridge within the zone of landfast sea ice off Barrow, Alaska. The ridge was linear in horizontal extent with level ice on either side, allowing for approximation by a two-dimensional (2D) model (Figure 1a). Figure 1b depicts the basic measurement configuration. Seven surface-NMR co-incident Tx-Rx loop locations (L0 - L6) were established across the ridge. All the important parameters for the measurements are listed in Table 1

The application of surface NMR to sea ice at Barrow is special for a number of reasons. The rough topography of the ridge and the large conductivity of seawater (~ 2.5 S/m) present a challenging situation for the forward modeling of EM fields and NMR sensitivities. The high variability of the earth's magnetic field $|B_0|$ at high latitudes on timescales of the same order as the measuring period causes off resonance effects which complicate the processing. Aside from such challenges, conditions

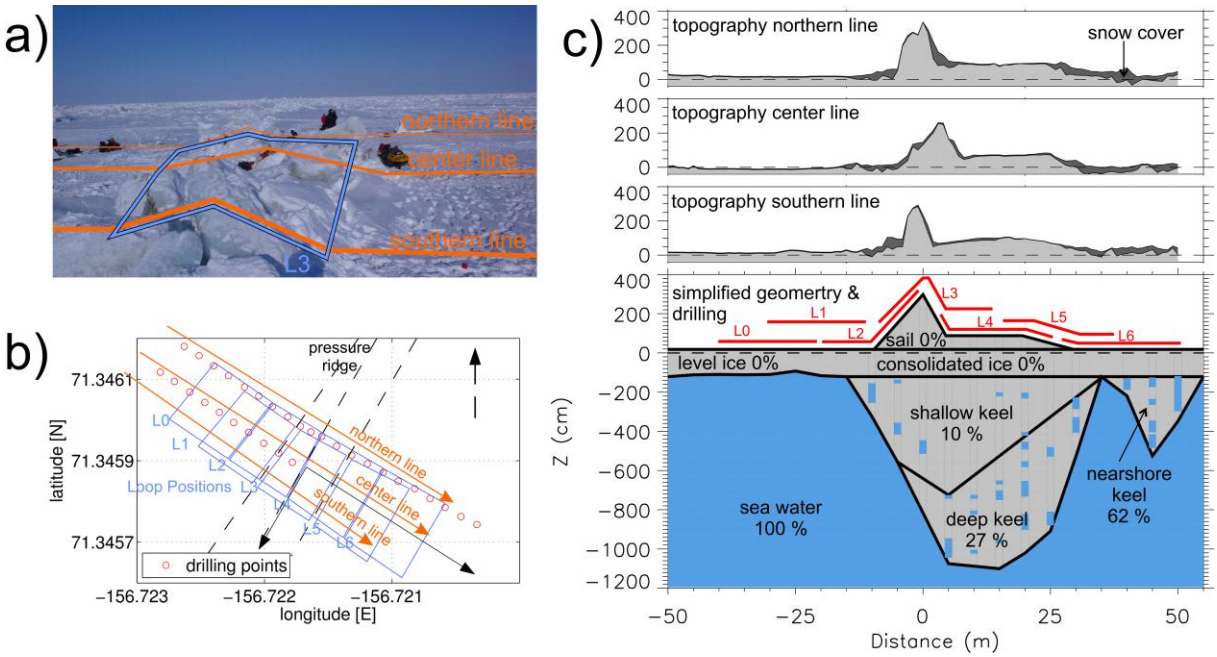

Figure 1: a) Photograph of the surveyed pressure ridge. The blue rectangle marks the position of loop L3; sea ice thickness and DGPS measurements were taken along the orange lines. b) Map of pressure ridge contours (dashed lines), loop positions (blue squares) and survey lines for DGPS and ice thickness measurements; along the center line an electrical resistivity profile was obtained. c) Topography measured along the three survey lines and simplified geometry based on topography and drill results; zero line is equivalent to water table; percentage values are water contents based on drill estimates; dashed line marks the water table; red lines the loop positions

in polar regions are favorable for surface-NMR measurements. High amplitudes of $|B_0|$ (~57 500 nT) and the large inclination angle of the B field (around 80°) increase the signal strength by about 25% compared to mid-latitudes (Hertrich, 2008). A strong signal is also expected due to the high subsurface water content. The remoteness of the survey site away from radio-frequency interference results in a very low noise level around 5 nV.

Auxiliary measurements of drilling, electrical resistivity tomography (ERT) and differential GPS were performed to constrain the inversion of surface NMR data with known ice thickness, electrical conductivity and topography. The locations of the NMR loops and the auxiliary measurements are shown and described in Figure 1b. A simplified geometry of the pressure ridge, based on drill holes and topography, is shown in Figure 1c and consists of 6 segments only.

Processing & Inversion

Initial processing of the data included the removal of obvious outliers on the measured NMR signal

Table 1: Surface NMR survey parameters

Date	April 5, 2011
Location	71.35° N, 156.72° W
Temperature	app. -20°C
Total magnetic field	57'457 +/- 30 nT
Inclination	80.5° +/- 0.1°
Declination	-1.75° +/- 0.5°
Larmor frequency	2445.7 - 2448.1 Hz
Instrument	Numis Poly[4]
Loop size	20 x 20 m
Configuration	coincident loops
Number of turns	2
Stacking rate	>=2
Pulse moments	0 - 9.5 As
Pulse length	0.04 s
Dead time	0.04 s
Acquisition time	1 s

[4]www.iris-instruments.com

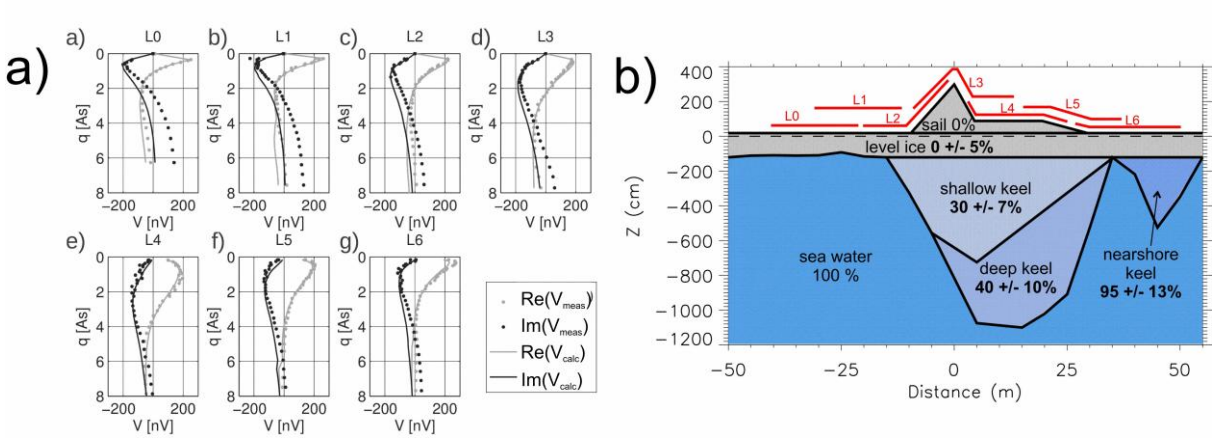

Figure 2: A) Real and imaginary parts of measured (dots) and calculated (solid lines) sounding curves for all seven loop positions. Calculated sounding curves are based on the best fit model shown in figure 2B. The imaginary part of loop 0 and loop 1 could not be fitted for larger pulse moments. The reason for this is the subject of further work. The mean RMS misfit between modeled and measured data of all loop positions is 20.3 nV for the real part and 47.8 nV for the imaginary part. **B)** Simplified geometry with inverted water contents. Errors were estimated by a forward propagation of the 5nV noise level through the calculations and by the standard deviation for a number of results based on different realistic conductivity models.

and least squares fitting to obtain the free induction decay (FID) of the NMR signal under considerations of off-resonance effects following Walbrecker et al. (2011) and relaxation during pulse following Walbrecker et al. (2009). The free induction decay conforms to the following formula:

$$V(t,q) = V(q)\cos[2\pi f_L(q)t + \phi_0(q)]e^{-t/T_2^*(q)}$$

where V is the measured voltage in the range of 10^{-9} Volts, q the pulse moment which is the product of current strength and pulse duration, f_L the Larmor frequency, t the time, ϕ_0 the phase (which incorporates instrument phase, conductivity induced phase and off-resonance shifts), and T_2^* the exponential decay. Resulting sounding curves for all loop positions showing $V(q)$ are displayed in Figure 2A (dotted lines). An increasing q increases the depth of investigation.

Forward modeling of the EM fields and inversion were carried out on the basis of the simplified geometry (Figure 1c). The conductivity values of level ice and sea water are reasonably well known from the analysis of an ice core and from oceanographic measurements. The governing equations describing the EM fields and the NMR sensitivities were solved on triangulated meshes and are detailed in Lehmann-Horn et al. (2012). They explicitly incorporate loop topography and conductivity anomalies within the subsurface.

With known NMR sensitivities the synthetic sounding curves could be calculated, and hence the measured sounding curves could be inverted to yield water contents of the 6 segments. The inversion was done using the algorithm developed by Lehmann-Horn et al. (2011). Measured and calculated sounding curves of the best fitted model are shown in Figure 2a and the inverted water contents are displayed in Figure 2b. The deduced water contents are independent of the starting values for the keel. However, crucial information is the conductivity distribution within the keel. Even when the conductivities of level ice and ocean water are known, the effective conductivity in the keel is only a conjecture, based on the Hashin-Shtrikman bounds. Therefore the inversion of the data was attempted for a series of different realistic keel-conductivity scenarios. The deviation between these different conductivity scenarios is reflected in the high error values of 10% in the deep keel and 7% in the shallow keel (Figure 2b). The even higher error of 13% in the near-shore keel is also attributed to low sensitivity coverage at the edge of the surveyed volume. Alternatively, results of the ERT survey (Figure 3) could serve as an input for the calculation of the EM fields. Unfortunately the shown resistivity distribution explains the measured ERT data only with an RMS error of 90 %, which is not reliable enough to use for the improvement of the surface NMR inversion. A major difficulty for the ERT work was the high contact resistances for electrodes on the sail, where large floe fragments of ice are electrically decoupled from the ocean-ice system by large voids of air.

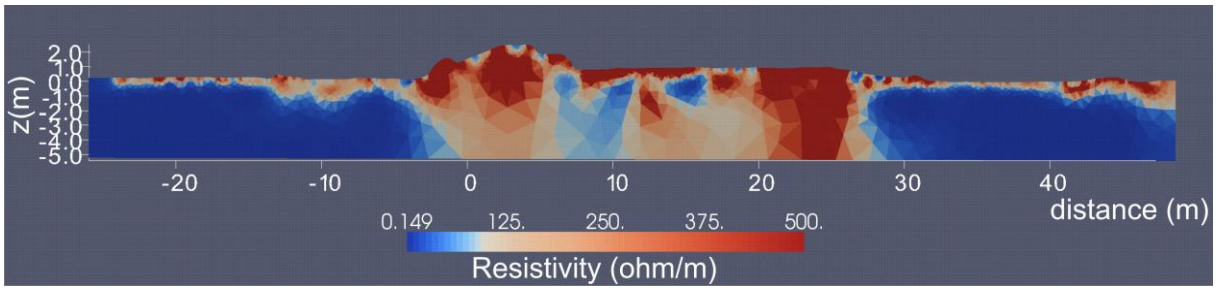

Figure 3: Inverted resistivity depth section over the pressure ridge for a 9-level Wenner array. The RMS misfit between model and data was about 90 % and therefore far too high for an incorporation into the surface NMR inversion.

The final estimated water contents of the deep and shallow keel, of 30% and 40% respectively, are higher than suggested from the drilling. This is reasonable since surface NMR signals emerge from water not only present in large cavities, but also in smaller pores. Another advantage of surface NMR is that it obtains volume integrated water contents in comparison to point-based measurements from drilling.

Conclusions & Outlook

Surface NMR has been successfully applied to obtain a rough distribution of the water content in an Arctic sea-ice pressure ridge. At the present time, deducing the ridge keel porosity from surface NMR requires auxiliary drilling to derive information about the keel geometry. Another challenge for future applications is to obtain reliable conductivity distributions in the keel as input for the calculation of the EM fields. Without reliable effective conductivity values for the keel, the water content data obtained from inversion will remain imprecise. However, the difficulty in obtaining ridge porosity data through other means and their importance in assessing the mass budget of the Arctic ice pack and potential sea-ice hazards in the context of maritime operations justify further work.

References

Hertrich, M. 2008. Imaging of groundwater with nuclear magnetic resonance. *Progress in Nuclear Magnetic Resonance Spectroscopy*, **53**(4), 227-248.

Lehmann-Horn, J. A., M. Hertrich, S. Greenhalgh and A. G. Green. 2011. Three-Dimensional Magnetic Field and NMR Anomalies and Variable-Surface Topography. *IEEE Transactions on Geoscience and Remote Sensing*, **49**(10), 1-14.

Lehmann-Horn, J. A., M. Hertrich, S. A. Greenhalgh and A. G. Green. 2012. On the sensitivity of surface NMR in the presence of electrical conductivity anomalies. *Geophysical Journal International*, **189**(1), 331-342.

Lehmann-Horn, J.A., Walbrecker, J.O., Hertrich, M., Langstone, G., MyClemont, A.F., Green, A.G. 2011 Imaging groundwater beneath a rugged proglacial moraine, *Geophysics*,**76**(5), B165-B172

Nuber, A., Rabenstein, L., Lehmann-Horn, J.A., Hertrich, M., Hendricks, S., Mahoney, A., Eicken, H., 2012, Water Content Estimates of a First-Year Sea Ice Pressure Ridge Keel from Surface Nuclear Magnetic Resonance Tomography. *Annals of Glaciology, submitted*

Walbrecker, J. O., M. Hertrich and A. G. Green. 2009. Accounting for relaxation processes during the pulse in surface NMR data. *Geophysics*, **74**(6), G27-G34.

Walbrecker, J. O., M. Hertrich and A. G. Green. 2011a. Off-resonance effects in surface nuclear magnetic resonance. *Geophysics*, **76**(2), G1-G12.